NASA TECHNICAL TRANSLATION

NASA TT F-14,962

CALCULATION OF POTENTIAL FLOW AROUND PROFILES WITH SUCTION AND BLOWING

K. Jacob

(NASA-TT-F-14962) CALCULATION OF POTENTIAL FLOW AROUND PROFILES WITH SUCTION AND BLOWING (Kanner (Leo) Associates) 34 p HC $3.75 CSCL 20D

N73-27209

Unclas

G3/12 09227

Translation of "Berechnung der Potentialströmung um Profile mit Absaugung und Ausblasen," Ingenieur-Archiv, Vol. 32, No. 1, 1963, pp. 51-65

NATIONAL AERONAUTICS AND SPACE ADMINISTRATION
WASHINGTON, D.C. 20546

JULY 1973

34 P8

STANDARD TITLE PAGE

1. Report No. NASA TT F-14,962	2. Government Accession No.	3. Recipient's Catalog No.
4. Title and Subtitle CALCULATION OF POTENTIAL FLOW AROUND PROFILES WITH SUCTION AND BLOWING		5. Report Date July 1973
		6. Performing Organization Code
7. Author(s) K. Jacob		8. Performing Organization Report No.
		10. Work Unit No.
9. Performing Organization Name and Address Leo Kanner Associates, P.O. Box 5187 Redwood City, California 94063		11. Contract or Grant No. NASw-2481
		13. Type of Report and Period Covered Translation
12. Sponsoring Agency Name and Address National Aeronautics and Space Administration, Washington, D.C. 20546		14. Sponsoring Agency Code

15. Supplementary Notes

Translation of "Berechnung der Potentialströmung um Profile mit Absaugung und Ausblasen," Ingenieur-Archiv, Vol. 32, No. 1, 1963, pp. 51-65.

16. Abstract

A method of computation has been developed for computing plane incompressible potential flows around arbitrary thick, cambered profiles with continuous or discontinuous blowing or suction. It works with source and vortex distributions on the contour and in the interior of the profile. An integral equation for the vortex distribution on the contour of the profile is arrived at, the solution of which is reduced to a linear set of equations. Finally, the method yields the velocity and pressure distribution on the contour of the profile and the flow-stream function for plotting the flow pattern. The practicability of the method was established for the circular cylinder by comparing the velocity distribution with the exact solution, and on some thick, cambered profiles by comparison of the theoretical pressure distribution with measurements.

17. Key Words (Selected by Author(s))	18. Distribution Statement Unclassified - Unlimited

19. Security Classif. (of this report) Unclassified	20. Security Classif. (of this page) Unclassified	21. No. of Pages 32	22. Price

NASA-HQ

CALCULATION OF POTENTIAL FLOW AROUND PROFILES WITH SUCTION AND BLOWING*

K. Jacob

1. Introduction /51**

For some time now, there have been investigations in aeronautical aerodynamics of flows around bodies where on a section of the surface liquids are being sucked off or blown out. Such flows play an important role, above all, in connection with problems of increased lift on airfoils. Thus, for instance, a separation of flow at large angles of incidence can be prevented on airfoils by means of sucking off of slowed-down boundary layer material or by tangential blowing out (energy supply into boundary layer); that way, maximum lift can be increased. During lift increase by suction, aside from the elimination of the boundary layer, the so-called sink effect plays a certain role. It is produced by superposing on the normal flow a flow (sink) directed in the form of a jet toward the place of suction. By this means, the pressure distribution on the profile is affected to a considerable extent. As an additional example of an application of blowing, the creation of very large coefficients of lift by means of so-called jet flaps should be mentioned.

---

*Abbreviated version of dissertation approved by the Faculty for Mechanical Engineering of the Institute of Technology, Braunschweig. Reviewer: Prof. Dr. H. Schlichting; Co-reviewers:Prof. Dr.-Ing. H. Peterman and Prof. Dr. R. Ludwig. The author wishes to thank Dr. F.W. Riegels, Göttingen, for the suggestion for this study and for valuable advice during its completion. The experiments were conducted in the Aerodynamic Testing Laboratory, Göttingen, with a subsidy from the German Research Association. The comprehensive version of this dissertation was submitted as an Internal Institute Report (60 A 43) to the Aerodynamic Testing Laboratory.

**Numbers in the margin indicate pagination in the foreign text.

To date, these problems have been chiefly investigated by experimental means.[1] There exist theoretical studies on the sink effect by F. Ehlers [1], C.B. Smith [2] and W.T. Lord [3]. In all of these studies, the conformal representation is used for calculating potential flow with suction, a method which is in general quite unwieldy. Theoretical studies on jet flaps by J.M. Davidson [4] and W. Jacobs [5] use the singularity method, but restrict themselves to thin profiles. It is desirable, therefore, to have a convenient method of calculation for potential flow around arbitrary profiles with arbitrarily distributed suction or outflow.

A method of this type is also desirable for another purpose, that of representing flow separations. A flow separation forms a so-called dead water, by means of which the external flow is forced away from the body. This results in a considerable change in flow pattern and pressure distribution around the body as compared to the flow adjoining it. This displacement effect can be determined as a calculated potential in accordance with a proposal by F.W. Riegels if the dead water is replaced by a quantity of fluid emitted from the profile. G. Jungclaus [6] has carried this out for a plane surface.

Additional contributions to a mathematically arrived-at potential calculation of plane flow separations have been made by R. Eppler [7]. He makes use of the conformal representation and seeks potential flows that possess constant pressure along free flow lines, that issue from two fixed points of separation and empty into two plates that are parallel to the initial direction of flow and that are located at some distance behind the body.[1]

[1] "The static pressure between these two flow lines (dead water pressure) is generally different from the static pressure of inflow."

This results in a two-parameter solution with the position of the points of separation and the dead water as free parameters.

For the purpose of calculating plane potential flow, there is also, besides the conventional method of conformal representation and singularity distribution on the wing chord, the possibility of profile contour distribution (vortices, sources, sinks). This method is the most suitable and elegant for arbitrary thick /52 profiles, a fact that had already been perceived by L. Prandtl [8] and W. Prager [9]. Lately, E. Martensen [10] and K. v. Sengbusch [11] have applied this method to single and grid profiles. Whereas Martensen deals with flows in which the normal component of velocity on the profile contour disappears (pure flow about a body), v.Sengbusch also admits normal component distributions (blowing and suction) that deviate from zero but are constant. The limiting to constant distribution of normal components is connected with the fact that in this case an exclusive distribution of singularities on the contour is being undertaken. If the distribution of normal components is discontinuous or even singular (single source), the tangential velocities as well as the vortex distributions become infinitely large at the points of discontinuity. However, this is quite troublesome for the numerical treatment of the problem.

However, such discontinuous distributions of the normal components are of special interest in some of the noted problems (e.g. suction through a slot). Therefore,it will be advantageous to try to split off the part of the tangential component containing infinity terms so that it can be represented analytically, leaving only a finite balance to be determined numerically. This splitting off can be managed in the following manner: the distribution of the normal component is represented by a corresponding distribution of sources on the contour and each boundary source is assigned a sink of half strength in the interior of the profile which is intended to receive the half of the source strength which flows inward. This sink should be placed near the source, but at a finite distance. It is now possible to calculate the normal and tangential components of the zone of each such source-sink arrangement and then to look for a vortex distribution on the contour that makes the normal components disappear except in the source itself. This normal component distribution, compensated for by the vortex distribution, is constant throughout, and its integral is zero. For this reason, the vortex distribution and tangential velocities of the field of vorticity remain finite (as long as the distance between source and sink does not become zero). The addition of the tangential components of the source-sink field and the vorticity field yields the unknown resultant tangential components. As a result, the infinitely large values are contained in the component of the source that can be rendered analytically. In consequence of transferring singularities (sinks) into the interior of the profile, a velocity remains in the interior of the profile, whereas it is zero for a singularity-free interior.

The method for calculating plane, incompressible potential flows around arbitrary thick, cambered profiles with arbitrary constant, discontinuous or singular suction or blowing, as presented in the following chapters, is based on this reasoning. For the time being, the method has only been worked out for flows around single profiles, but it can also be expanded to encompass grid flows.

Applying the method to suction flows does not present any difficulties. However, for using the method for profiles with jet flaps, an expansion of the method would be required so that not only the profile contour but also the jet boundaries would receive a vortex distribution. Not knowing its location,to begin with, does in this case present a certain difficulty. The possibility of an approximate representation of flow separations is a special advantage of this method. In order to determine the position, distribution and strength of a given source distribution, the points of separation and limiting conditions for dead water boundaries must be known. The points of separation can be obtained by means of boundary calculations. The fact that a nearly constant pressure prevails in the dead water can be utilized as a condition for dead water limits. G. Jungclaus and R. Eppler also made use of this fact, substantiated by measurements. In contrast to the noted Eppler procedure, dead water pressure as a free parameter is not applicable to our method because we limit ourselves to potential flows in which there are no singularities outside the profile. The proposed method is connected with some calculating effort which, however, can readily be accomplished by the use of an electronic computer. The method of computation is first set forth in the following. Some remarks on the various applications and calculated examples follow.

2. The Basic Concept of the Computing Method /53

The plane incompressible potential flow is to be calculated for a specified thick, cambered profile with a uniformly curved contour on which, at an arbitrary part of the contour, a liquid disappears or is emitted, corresponding to a specified continuous, discontinuous, or singular source distribution on the contour.

A simple special form of such a flow can be exactly calculated in a very simple manner. Given a source of strength +E and a sink of strength -E/2 at a distance R, a flow is produced around a circle of radius R in whose center is the sink and on whose contour the source is located (Fig. 1a). This furnishes us with the simplest form of a plane potential flow around a thick body where a liquid is emitted or -- with reversal of signs -- enters. Half of the liquid emitted by the source flows outward into

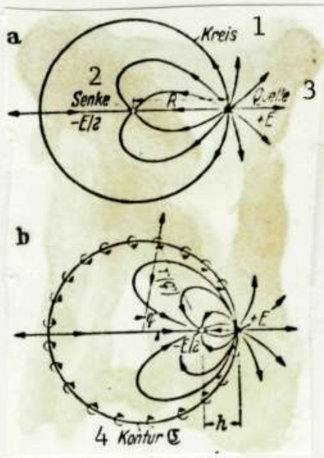

Fig. 1. Drawing depicting outflow on a circular cylinder. a) Sink at center of circle; b) Sink not in center and vortex distribution on contour.

Key: 1. Circle
2. Sink
3. Source
4. Contour

infinity, the other half is absorbed by the sink located in the interior.

However, it is also possible to arrive at the same external flow by locating the sink not in the center of the circle but somewhere on the inside of the circle at a finite distance h from the source (Fig. 1b), and by means of an added vortex distribution of the contour make all velocity components on the contour, normal to the contour, disappear except the infinite one at the point of the source itself. Such a vortex distribution does exist and is finite and continuous throughout, but only if the normal components to be eliminated $w_n(s)$ are distributed over the contour (working length s) in a continuous manner and in a form allowing continuous integration and if the integral over the entire normal component distribution of profile contour C, which must be eliminated, disappears; that is, if the following holds:

$$\int_{\mathfrak{C}} w_n(s)\,ds = 0 \qquad (1)$$

However, these requirements are met in this case: the normal component induced by the source is constant, i.e., $w_{n\rho} = E/4\pi R$, the normal component originating from the sink is constant on account of the finite distance $r(\phi)$, and Eq. (1) is also satisfied because the sink absorbes just the amount of liquid delivered by the source to the interior.

The latter method (sink somewhere in interior of profile) can also be applied to arbitrary thick profiles with uniformly curved contour. It is true that the normal velocity on the contour induced by the source is no longer constant, but it is uniform; because close to the source the equation still holds; $w_{n\rho} = E/4\pi R$, in which case R is now the radius of curvature of the profile at the location of the source. The following must be well understood: at the location of the source itself, the normal velocity is of course infintely large and it can not and may not be eliminated by the continuous vortex distribution. In the vicinity of the source, the vortex distribution should only compensate for the velocity $w_{n\rho} = E/4\pi R$ and the effect of the sink, thereby causing the contour of the profile to remain arbitrarily close to the source as the contour of the profile.

In place of the single source at one point of the contour, it is also possible to assume many elementary sources as existing closely spaced on the contour, i.e., a source distribution on one part of the contour. In principle, this does not change the solvability of the problem.

The principal item of the procedure is the determination of the vortex distribution. The starting point is the vortex element $d\Gamma = \gamma_k(s)ds$ lying on the contour of the profile. At a point P(x, y) of the flow field, at a distance r from the vortex element (Fig. 2), it furnishes for flow-stream function ψ the following part:

$$d\Psi = \frac{-d\Gamma}{2\pi}\ln r = \frac{-\gamma_k(s)\,ds}{2\pi}\ln r = \frac{\gamma_k(s)}{2\pi}\left(\ln\frac{1}{r}\right)ds\,;$$

where positive $\gamma_k(s)$ corresponds to a vortex rotating counterclockwise.

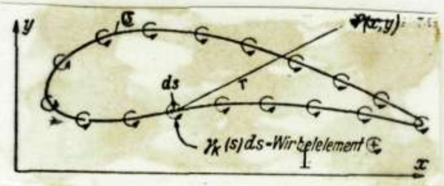

Fig. 2. Drawing for setting up the integral equation for the vortex distribution on the contour of the profile.

Key: 1. Vortex element

Integration over the entire contour of the profile C then furnishes the following at point P(x, y) for the flow-stream function:

$$\Psi(x, y) = \frac{1}{2\pi} \int_{\mathfrak{C}} \gamma_k(s) \ln \frac{1}{r(s, x, y)} ds . \qquad (2)$$

The derivation of the flow-stream function in the direction of the profile tangent $\partial\Psi/\partial t$ is the normal component of velocity induced by the vortex distribution: /54

$$w_{n\gamma} = \frac{\partial \Psi}{\partial t} .$$

The normal component $w_{n\rho}$, on the contour of the profile, induced by the given source and sink distribution, shall be opposite and equal to:

$$-w_{n\gamma} = -w_{n\varrho s} \quad \text{on } \mathfrak{C}$$

or

$$\left(\frac{\partial \Psi}{\partial t}\right)_{\mathfrak{C}} = \frac{1}{2\pi} \frac{\partial}{\partial t} \int_{\mathfrak{C}} \gamma_k(s') \ln \frac{1}{r(s', s)} ds' = -w_{n\varrho s}(s) . \qquad (3)$$

$w_{n\rho s}$ is here again understood not to contain the normal velocity $\rho(s)/2$ which is supplied by the elementary source $\rho(s)ds$ at the location s itself.

Thus, (3) yields a first order integral equation for vortex distribution $\gamma_k(s)$. It can be converted to one of second order with a continuous kernel throughout, which is necessary for a numerical treatment. If now the integral is replaced by a sum, the result is a linear set of equations, the reduction of which yields the unknown vortex distribution.

The tangential velocities induced by the sources, sinks and vortices at each contour point can now be calculated and added; it is now also possible to calculate the value of the flow function at each point of the flow field. The velocities yield the pressure distribution on the profile; the flow function values provide the sign of the flow pattern.

At first, there is a pure discharge or suction flow around the profile (Fig. 3d). It can then be superposed (Fig. 3e) with translation and circulation flows which can be calculated in accordance with Martensen.

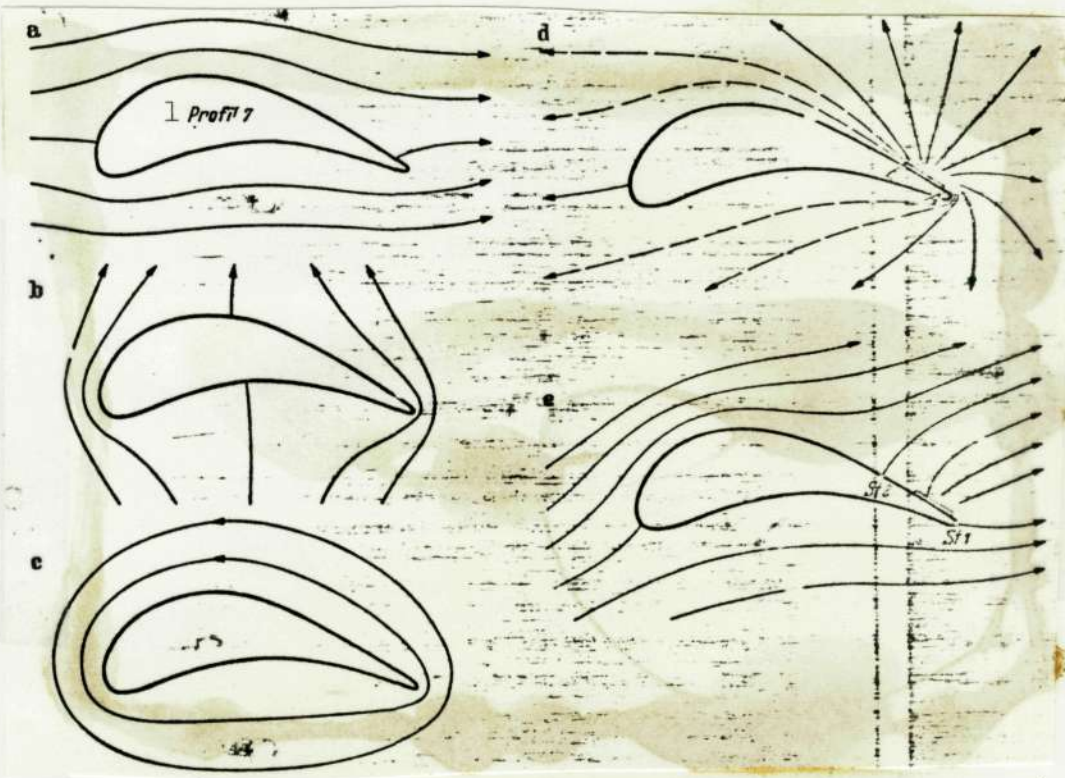

Fig. 3. Calculated flow patterns for a thick profile.
[Continued on following page.]

Fig. 3 (cont'd.). a) 1. Basic flow: $W_\infty = 1$, $\alpha = 0°$; $\Gamma = 0$; b) 2. Basic flow: $W_\infty = 1$; $\alpha = 90°$; $\Gamma = 0$; c) 3. Basic flow: $W_\infty = 0$, $\Gamma = 2\pi$; d) A pure outflow with constant source distribution $q(\phi)$ = const from A to E; e) Superposition of flow in [illegible] 2a to 2d for $\alpha = 20°$ and separation at St1 and St2.

Key: 1. Profile

3. Method of Calculation

The following is the preparation of the formulas necessary for practical calculations.

a) Single Source on the Contour of the Profile /55

First, the case of the single source (index Q) with corresponding single sink of half force in the interior of the profile (index S) is dealt with. The variations in the formulas resulting from conversion to continuous source distribution are given in Section 3b.

Transformation of the Integral Equation

Equation (3) is an integral equation of the first degree with singular kernel and, therefore, unsuitable for practical calculation. However, it can be transformed into an integral equation of the second degree with overall continuous kernel. This is done in accordance with the above-mentioned study by E. Martensen, where an integral equation occurs which differs from (3) only by the right side of it.

A parametric representation $x(\phi)$ and $y(\phi)$ is introduced for the profile contour; it is assumed that $x(\phi)$ and $y(\phi)$ are periodically and twice continuously differentiable and that the profile contour will rotate exactly once counterclockwise for $\phi = 0$ to 2π. In addition, for $dx/d\phi = \dot{x}(\phi)$, $dy/d\phi = \dot{y}(\phi)$, $\dot{x}(\phi)^2 + \dot{y}(\phi)^2 \neq 0$ must always exist so that at each point a tangential unit vector

$$\mathfrak{t} = \frac{1}{\sqrt{\dot{x}(\varphi)^2 + \dot{y}(\varphi)^2}} \begin{Bmatrix} \dot{x}(\varphi) \\ \dot{y}(\varphi) \end{Bmatrix}$$

can be defined.

In addition, a transformed circulation distribution $\gamma(\phi)$ is introduced by means of the defining equation

$$\gamma(\varphi)\, d\varphi = \gamma_k(s)\, ds \qquad \text{or} \qquad \gamma_k = \frac{\gamma(\varphi)}{ds/d\varphi} = \frac{\gamma(\varphi)}{\sqrt{\dot{x}(\varphi)^2 + \dot{y}(\varphi)^2}}. \tag{3a}$$

Now, the integral equation (3), after some intermediate calculation, can be converted to

$$\gamma(\varphi) - \frac{1}{2\pi}\int_0^{2\pi} L(\varphi,\psi)\,\gamma(\psi)\, d\psi = \frac{1}{\pi}\int_0^{2\pi} w_{nQS}(\psi)\sqrt{\dot{x}(\psi)^2 + \dot{y}(\psi)^2}\,\operatorname{ctg}\frac{\psi-\varphi}{2}\, d\psi \tag{4}$$

with

$$L(\varphi,\psi) = 1 - \frac{1}{2\pi}\int_0^{2\pi} H(\varkappa,\varphi)\operatorname{ctg}\frac{\varkappa-\varphi}{2}\, d\varkappa \tag{4a}$$

and

$$H(\varkappa,\psi) = 2\,\frac{[x(\varkappa)-x(\psi)]\,\dot{x}(\varkappa) + [y(\varkappa)-y(\psi)]\,\dot{y}(\varkappa)}{[x(\varkappa)-x(\psi)]^2 + [y(\varkappa)-y(\psi)]^2} - \operatorname{ctg}\frac{\varkappa-\psi}{2} \quad \text{für} \quad \varkappa \neq \psi \tag{4b}$$

and as limiting value

$$\lim_{\psi\to\varkappa} H(\varkappa,\psi) = \frac{\dot{x}(\varkappa)\,\ddot{x}(\varkappa) + \dot{y}(\varkappa)\,\ddot{y}(\varkappa)}{\dot{x}(\varkappa)^2 + \dot{y}(\varkappa)^2}.$$

Moreover, it can be proven that the following holds true:

$$\int_0^{2\pi} H(\varkappa,\psi)\, d\varkappa = 0. \tag{4c}$$

This relationship, after transition to a finite score, can subsequently be used for calculating the limiting value of H as a negative sum of the remaining values of H. That way, it is possible to avoid second derivatives that can give rise to inaccuracies when using numerical computations.

The integral equation (4) is a Fredholm integral equation of the second order with overall continuous kernel and is solvable, as has been shown by Martensen.

Linear Set of Equations for Computing Outflow

For the purpose of numerical computation, the profile at 2N shall be given in ϕ equidistant contour points $P_\mu(x_\mu, y_\mu)$ with $\phi_\mu = \mu \cdot 2\pi/2N$ and $\mu = 0, 1, \ldots (2N - 1)$.

Using the simple quadrilateral formula for the numerical integration of the left side of (4) and a formula given by Martensen for the numerical computation of the cotangent integral in (4) and (4a), the following linear set of equations for determining the vortex distribution is finally arrived at:

$$\gamma_\mu - \frac{1}{2N} \sum_{\nu=0}^{2N-1} L_{\mu\nu} \gamma_\nu = 2 \sum_{\nu=1}^{2N-1} A_\nu J_{\mu+\nu} \qquad (5)$$

with

$$\mu = 0, 1, 2 \ldots (2N - 1),$$

$$A_\nu = \frac{1-(-1)^\nu}{2N} \operatorname{ctg} \frac{\varphi_\nu}{2}, \qquad \varphi_\nu = \nu \frac{2\pi}{2N}, \qquad (5a)$$ /56

$$J_\mu = (\Gamma_{\kappa Q S})_\mu \sqrt{\dot{x}_\mu^2 + \dot{y}_\mu^2}, \qquad (5b)$$

$$L_{\mu\nu} = 1 - \sum_{\kappa=1}^{2N-1} A_\kappa H_{\mu+\kappa,\nu}, \qquad (5c)$$

$$H_{\mu\nu} = 2 \frac{(x_\mu - x_\nu)\dot{x}_\mu + (y_\mu - y_\nu)\dot{y}_\mu}{(x_\mu - x_\nu)^2 + (y_\mu - y_\nu)^2} - \operatorname{ctg} \frac{(\mu - \nu) 2\pi}{4N} \quad \text{für} \quad \mu \neq \nu \qquad (5d)$$

and in accordance with (4c)

$$H_{\nu\nu} = -\sum_{\substack{\mu=0\\ \mu\neq\nu}}^{2N-1} H_{\mu\nu} \quad \text{for } \mu = \nu$$

The derivatives of the coordinates with respect to ϕ, required for (5b) and (5d), are easily derived in accordance with Martensen from the formulas

$$\dot{x}_\mu = \sum_{\nu=1}^{2N-1} B_\nu x_{\mu+\nu}, \quad \dot{y}_\mu = \sum_{\nu=1}^{2N-1} B_\nu y_{\mu+\nu} \quad \text{with} \quad B_\nu = \frac{(-1)^{\nu+1}}{2} \operatorname{ctg} \frac{\varphi_\nu}{2}. \tag{5e}$$

Finally, also required for (5b) are the normal components $(w_{n\rho S})_\mu$, induced by source and sink at contour points $P_\mu(x_\mu, y_\mu)$. As shown in the comprehensive version of this study, the following formula is arrived at:

$$(w_{nQS})_\mu = (w_{nQ})_\mu + (w_{nS})_\mu \tag{6}$$

with

$$(w_{nQ})_\mu = \frac{E}{2\pi\sqrt{\dot{x}_\mu^2 + \dot{y}_\mu^2}} \frac{(x_\mu - x_Q)\dot{y}_\mu - (y_\mu - y_Q)\dot{x}_\mu}{(x_\mu - x_Q)^2 + (y_\mu - y_Q)^2} \quad \text{for } P_\mu \neq P_Q$$

and as limiting value in accordance with l'Hospital

$$(w_{nQ})_\mu = \frac{E}{2\pi\sqrt{\dot{x}_\mu^2 + \dot{y}_\mu^2}} \frac{\dot{x}_\mu \cdot \ddot{y}_\mu - \dot{y}_\mu \cdot \ddot{x}_\mu}{2(\dot{x}_\mu^2 + \dot{y}_\mu^2)} \quad \text{for } P_\mu \equiv P_Q \tag{6a}$$

and

$$(w_{nS})_\mu = \frac{-E/2}{2\pi\sqrt{\dot{x}_\mu^2 + \dot{y}_\mu^2}} \frac{(x_\mu - x_S)\dot{y}_\mu - (y_\mu - y_S)\dot{x}_\mu}{(x_\mu - x_S)^2 + (y_\mu - y_S)^2}. \tag{6b}$$

For this, x_ρ, y_ρ or x_S, y_S are the coordinates of source or sink, and E is the strength of the source.

In order to make the set of equations (5) unique, it is still necessary to determine the total circulation. For a given position and strength of a source, there are an infinite number of outflows around the specified body, depending on how large the total circulation is. Therefore, we add the condition that the total circulation shall be zero:

$$\Gamma = \oint_{\mathfrak{C}} \gamma_k(s)\, ds = \int_0^{2\pi} \gamma(\varphi)\, d\varphi \approx \frac{2\pi}{2N} \sum_{\nu=0}^{2N-1} \gamma_\nu = 0 \tag{7}$$

and in consequence, we omit any of the 2N equations of (5). The set of equations now yields the vortex distribution on the contour of the profile which jointly with the source-sink flow results in a circulation-free potential flow around the specified profile, while at the point of the source there occurs a source-like outflow.

The tangential velocity at the outer border of the contour at point P_μ is composed of the portion originating in the source-sink flow and the portion originating in the vortex distribution:

$$(w_t)_\mu = (w_{tQS})_\mu + (w_{t\gamma})_\mu \,. \tag{8}$$

These portions result in (cf. the comprehensive version):

$$(w_{tQS})_\mu = \frac{E}{2\pi\sqrt{\dot{x}_\mu^2 + \dot{y}_\mu^2}} \left(\frac{(x_\mu - x_Q)\,\dot{x}_\mu + (y_\mu - y_Q)\,\dot{y}_\mu}{(x_\mu - x_Q)^2 + (y_\mu - y_Q)^2} - \frac{1}{2}\, \frac{(x_\mu - x_S)\,\dot{x}_\mu + (y_\mu - y_S)\,\dot{y}_\mu}{(x_\mu - x_S)^2 + (y_\mu - y_S)^2} \right) \tag{8a}$$

and /57

(8b)

$$(w_{t\gamma})_\mu = \frac{1}{\sqrt{\dot{x}_\mu^2 + \dot{y}_\mu^2}} \left(\frac{\gamma_\mu}{2} + \frac{1}{2N} \sum_{\nu=0}^{2N-1} \gamma_\nu K_{\mu\nu} \right)$$

with

$$K_{\mu\nu} = \frac{(x_\mu - x_\nu)\,\dot{y}_\mu - (y_\mu - y_\nu)\,\dot{x}_\mu}{(x_\mu - x_\nu)^2 + (y_\mu - y_\nu)^2} \qquad \text{für} \qquad \nu \neq \mu$$

and

$$K_{\nu\nu} = N - \sum_{\substack{\mu=0 \\ \mu\neq\nu}}^{2N-1} K_{\mu\nu} \qquad \text{für} \qquad \nu = \mu \,.$$

Superposition of Pure Outflow with Translation and Circulation Flow

As has been shown by Martensen, it is possible also to compute other flows around the profile (without blowing) by means of the set of equations (5) (Fig. 3a-c) if the right side is changed.

For the so-called first basic flow (parallel flow in x direction with flow velocity $W_\infty = 1$, circulation $\Gamma = 0$, angle of attack against the x axis $\alpha = 0$) the right sides are:

$$R_{a\mu} = 2 \sum_{\nu=1}^{2N-1} A_\nu \dot{y}_{\mu+\nu}$$

with A_ν from (5a).

For the second basic flow (parallel flow in y direction with $W_\infty = 1$, $\Gamma = 0$, $\alpha = 90°$) the following holds:

$$R_{b\mu} = -2 \sum_{\nu=1}^{2N-1} A_\nu \dot{x}_{\mu+\nu},$$

For the third basic flow (pure circulation flow with $W_\infty = 0$, $\Gamma = 2\pi l \cdot 1$ where l is the depth of the profile) the following applies

$$R_{c\mu} = 0$$

And in (7) the following must be substituted:

For the first basic flow: $\Gamma = 0$

For the second basic flow: $\Gamma = 0$

For the third basic flow: $\Gamma = 2\pi l \cdot 1$.

The resulting γ_a, γ_b, γ_c then yield directly by way of (3a) the so-called basic velocities[2] w_a, w_b, w_c; these are then relative

[2]Martensen has shown that for basic flows without blowing, the vortex distribution γ_k is identical with the tangential velocity at the outer border of the contour because the velocity is zero everywhere in the interior of the profile.

to W_∞ or $\Gamma/2\pi l$. It is now easy to calculate compound flows by means of simple superposition (Fig. 3). The compound tangential velocity at the contour of the profile at point P_ν is

$$\frac{w_\nu}{W_\infty} = a(w_a)_\nu + b(w_b)_\nu + c(w_c)_\nu + g(w_t)_\nu . \tag{9}$$

For this, the so-called superposition factors are

$$a = \cos\alpha , \tag{9a}$$
$$b = \sin\alpha , \tag{9b}$$
$$c = \frac{\Gamma}{2\pi l \cdot 1} = -\frac{c_a}{4\pi} . \tag{9c}$$

The superposition factor g results in the following if in the computation of w_t strength $E = 2\pi l \cdot 1$

$$g = \frac{E}{2\pi l \cdot 1} \tag{9d}$$

A negative g results in an outflow instead of a suction flow.

If for compound flow, stagnation points are assumed to exist at certain locations on the profile, the condition there must be $w_\nu = 0$, i.e.,

$$\left.\begin{aligned} a(w_a)_{St1} + b(w_b)_{St1} + c(w_c)_{St1} + g(w_t)_{St1} = 0 ,\\ a(w_a)_{St2} + b(w_b)_{St2} + c(w_c)_{St2} + g(w_t)_{St2} = 0 ,\end{aligned}\right\} \tag{9e}$$

in which case the indices St1 and St2 indicate the points of stagnation, i.e., $(w_a)_{St1}$, etc. are the values of the basic velocities at the points of the profile where the stagnation points are supposed to be located. If the angle of attack α is given, that is, if a and b are fixed, Eqs. (9e) will then yield c and g. /58

Flow-Stream Function, Flow Pattern

In order to be able to plot the flow pattern, the flow-stream function Ψ must be calculated at many points of the flow field. Equation (2) furnishes the portion of a vortex distribution for the flow-stream function at point P(x, y)

$$\Psi_\gamma(x,y) = \frac{1}{2\pi} \int_{C_s} \gamma_s \ln \frac{1}{r}\, ds\,.$$

By using (3a) and $r = \sqrt{[x - x(\phi)]^2 + [y - y(\phi)]^2}$ and integration in accordance with the rectangular formula, the following formula is obtained

$$\Psi_\gamma(x,y) = -\frac{1}{2}\,\frac{1}{2N} \sum_{\mu=0}^{2N-1} \gamma_\mu \ln\left[(x - x_\mu)^2 + (y - y_\mu)^2\right]. \qquad (10a)$$

The portion originating in source and sink is

$$\Psi_{QS}(x,y) = \frac{E}{2\pi}\,\alpha_Q - \frac{E/2}{2\pi}\,\alpha_S \qquad (10b)$$

with α_ρ = arctan $[(y - y_\rho)/(x - x_\rho)]$ and α_S = arctan $[(y - y_S)/$ $/(x - x_S)$, where α lies between 0 and 2π depending on the sign of Δy and Δx.

For superposition of parallel flows with $W_\infty = 1$, the following is added:

$$\Psi_a(y) = y \quad \text{and} \quad \Psi_b(x) = -x\,. \qquad (10c)$$

In case of superposition of the three basic flows and the outflow with the factors a, b, c, g, the following applies:

$$\Psi(x,y) = a\,[\Psi_a(y) + \Psi_{\gamma a}(x,y)] + b\,[\Psi_b(x) + \Psi_{\gamma b}(x,y)] + c\,\Psi_{\gamma c}(x,y) + g\,[\Psi_{QS}(x,y) + \Psi_{\gamma QS}(x,y)]\,. \qquad (11)$$

b) Transition to Continuous Source Distribution

It is possible to proceed in accordance with the same principle as for a single source when dealing with a case of continuous source distribution $q(\phi)$ on a section of the contour. For this, it is necessary to place many elementary sources on the "source line" of the profile and to assign an elementary sink of half strength to each elementary source which might lie at a distance h on the normal, oriented toward the interior of the profile. The normal components $(w_{nqs})_\mu$, induced by the source and sink distribution, will yield the right sides of the set of equations (5). In all other respects, the computation is exactly the same as before.

Location and form of source distribution must be given for calculating w_{nqs} and w_{tqs}. The source line is to be in the form

$$x_q(\varphi) = a_0 + a_1\varphi + a_2\varphi^2 + \cdots + a_m\varphi^m, \qquad y_q(\varphi) = b_0 + b_1\varphi + b_2\varphi^2 + \cdots + b_m\varphi^m. \tag{12a}$$

The polynomial coefficients can be determined from linear sets of equations by means of m + 1 contour points $P_\mu(x_\mu, y_\mu)$ given in the area of the source section. In that case, the coordinates of the associated elementary sinks are [12]:

$$x_s(\varphi) = x_q(\varphi) - h\,\frac{\dot{y}_q(\varphi)}{\sqrt{\dot{x}_q(\varphi)^2 + \dot{y}_q(\varphi)^2}}, \qquad y_s(\varphi) = y_q(\varphi) + h\,\frac{\dot{x}_q(\varphi)}{\sqrt{\dot{x}_q(\varphi)^2 + \dot{y}_q(\varphi)^2}}. \tag{12b}$$

The normal component $d(w_{nqs})_\mu$ induced at contour point P_μ by the elementary source $q(\phi)d\phi$ and the elementary sink $-\frac{1}{2}q(\phi)d\phi$ belonging to it can be determined in accordance with (6) and integrated over the source section.

In the same manner, the tangential velocity in P_μ can be arrived at by integration of the components of $d(w_{tqs})_\mu$ which is calculated in accordance with (8a).

The right sides of the set of equations (5) can then be calculated by means of $(w_{nqs})_\mu$. The solution yields $(\gamma_{qs})_\mu$ and (8b), once again $(w_{t\gamma})_\mu$. When computing $(w_t)_\mu$ in accordance with (8), $(w_{tqs})_\mu$ now replaces $(w_{tQS})_\mu$.

The following replaces (10b) for computing the flow-stream /59 function $\Psi_{qs}(x, y)$:

$$\Psi'_{qs}(x, y) = \frac{1}{2\pi} \int_{\varphi_A}^{\varphi_E} q(\varphi) \left(\operatorname{arctg} \frac{y - y_q(\varphi)}{x - x_q(\varphi)} - \frac{1}{2} \operatorname{arctg} \frac{y - y_s(\varphi)}{x - x_s(\varphi)} \right) d\varphi . \tag{13}$$

4. Examples of Computations, Applications

First, the procedure should undergo a test by comparing the velocity distribution with the exact solution for the circular cylinder with point blowing. Furthermore, the practicability of the method will be made plausible by showing that "plausible" velocity distributions and flow patterns emerge for a rather common profile, first, for pure outflows and, finally, also for superpositions with parallel and circulation flows. Results are to be considered as "plausible" when they can be anticipated, at least qualitatively, in accordance with the potential theory. Finally, some possible applications of the method will be discussed, namely the computation of flows with suction, of flow separations and of flows around airfoils with jet flaps. Some comparisons with measurements are also carried out for flow separations. The computations are always made with 2N = 36 plotted points. The most important data of the examples of computations are given in the illustrations.

a) Circular Cylinders with Single Sources

As shown in the comprehensive version, the following applies exactly as shown to the circular cylinder with point outflow (Fig. 1a):

$$w_t(\varphi) = \frac{Q}{2\pi R} \operatorname{ctg} \frac{\varphi - \varphi_Q}{2}, \tag{14}$$

where Q = E/2 represents the quantity flowing to the outside, R is the radius, and $\phi - \phi_Q$ represents the angle at the center between the contour point under consideration and the source point.

In order to see whether the method under consideration (Fig. 1b) would yield the same results and how much the distance of the sink from the source h/R would affect the accuracy of the results, a computation for a single source +E at $\phi_Q = 45°$ and with a sink -E/2 at various distances h/R was carried out. The greatest deviations are found at the (greatest) values in the vicinity of the source. The relative deviations for this region /60 are given in Table 1. The relative deviations are already in all cases smaller than 1% at h/R = 0.2 and diminish with increasing h/R. At a very small h/R, the results oscillate around the exact solution. A changeover to a larger number of plotted 2N points or simply a smoothing-out should still give good results, even at h/R = 0.1 (Fig. 4).

TABLE 1. RELATIVE DEVIATIONS OF TANGENTIAL COMPONENTS FROM EXACT VALUE FOR THE CIRCULAR CYLINDER WITH SINGLE SOURCE (ϕ_ρ = 45°); h = DISTANCE OF SINK -E/2 FROM SOURCE +E; COMPARE FIGURE 4.

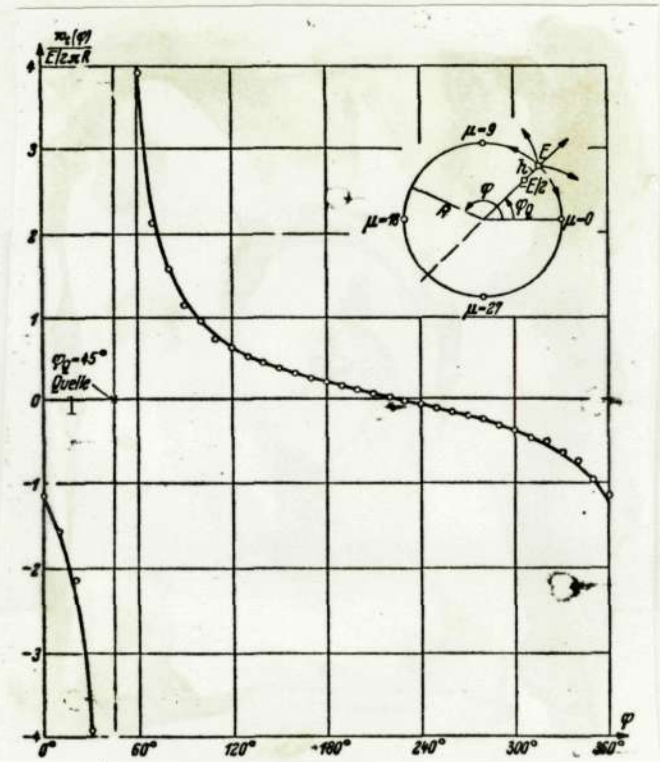

Fig. 4. Velocity distribution for pure outflow around the circular cylinder with a source having strength E on the contour at $\phi_Q = 45°$. ——: exact solution in accordance with Eq. (14); O: method under consideration with h/R = 0.1.

	$\left\lvert \frac{w_t - w_{t\,exact}}{w_{t\,exact}} \right\rvert$ for		
	h/R = 0,1	h/R = 0,2	h/R [illegible]
40° and 50°	0,081	0,006	0,00[illegible]
30° and 60°	0,032	0,008	0,00[illegible]

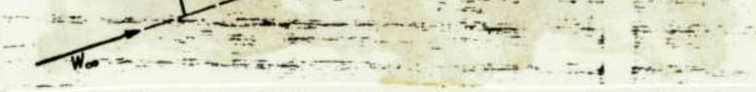

Fig. 5. Profile 7, shape and selected point distribution.

b) Profiles with Source Distributions

To begin with, additional calculations were based on the thick, cambered profile (profile 7) represented in Fig. 5. In addition, continuous source distributions were now used in place of the single source. Profiles NACA 2412 and Gö 801 were used for comparison with measurements.

Figure 6 shows the flow pattern and Fig. 7 the velocity distribution for a pure source flow with constant source distribution on a section of the contour; they are the outcome of proceeding in accordance with the method under consideration. Both appear to be quite "plausible."

For a practical application, it is now necessary /61
to superpose the circulation-free pure flow due to blowing with translation and circulation flows in

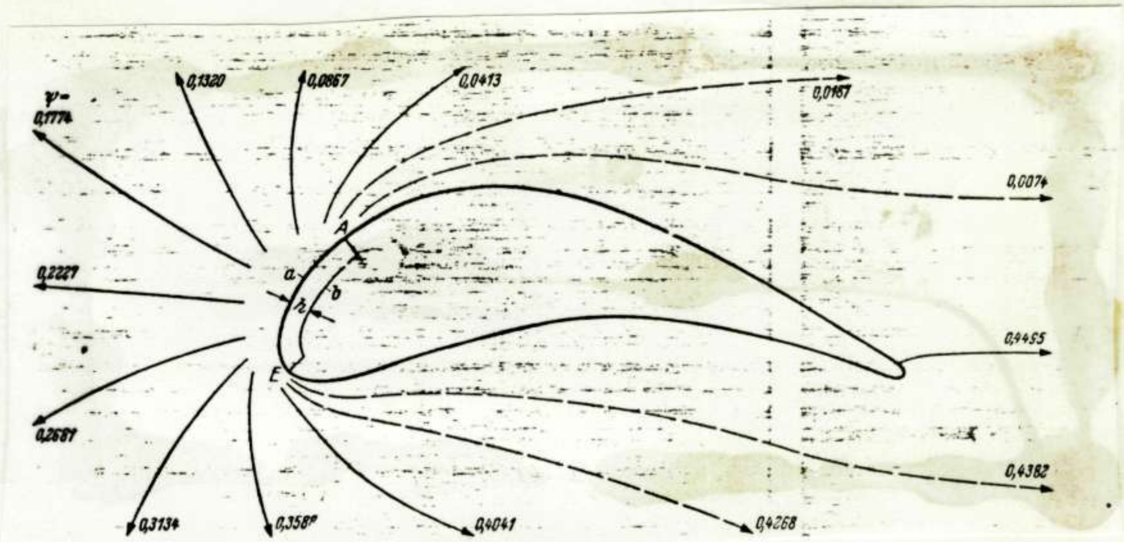

Fig. 6. Calculated flow pattern for a pure outflow around profile 7 at constant source distribution $q(\phi) = 1$ from A to E, distance of sink $h/l = 0.035$. a. Source line; b. sink line.

such a way that certain specified conditions relative to initial direction of flow, stagnation point, quantity of outflow or suction, jet boundary, circulation, etc., are being fulfilled. It is never possible to specify more than a few quantities. It can be seen from formulas (9a) to (9e) that all superposition factors are fixed if three of the quantities α, Γ, E, St1 and St2 are given, as long as a certain form and position of source distribution are used as a basis. Form and position of source distribution offer additional degrees of freedom to be skillfully utilized for certain objectives (e.g. representation of a flow separation).

Flow with Suction /62

Form and position of source distribution on the profile and the entire quantity -E to be sucked off are given in case of a flow with suction. Added to this are Kutta's outflow conditions for the location of the rear stagnation point and, of course, the given angle of attack α. Given this, all superposition factors can be calculated.

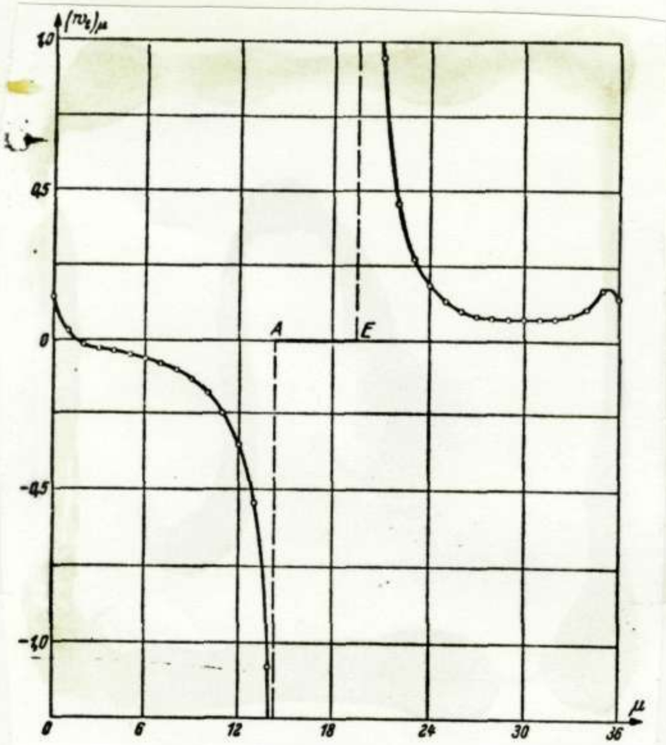

Fig. 7. Velocity distribution for a pure outflow around profile 7 at constant source distribution $q(\phi) = 1$ from A to E (see also Fig. 6) and sink distance $h/l = 0.035$. μ = number of points (see Fig. 5).

A flow with suction in the vicinity of the leading edge of the profile was calculated for profile 7 (Fig. 8). For this, a sink distribution $q(\phi)$ = const with the location specified in Fig. 8, having the quantity coefficient $c_Q = Q/(W_\infty \cdot l) = -0.10$ was selected; the rear stagnation point lies at $\mu = 0$ and the angle of attack is $\alpha = 10°$. Figure 8 shows the flow pattern and Fig. 9 the pressure distribution with and without suction. Figure 9 clearly indicates the lowering of the suction

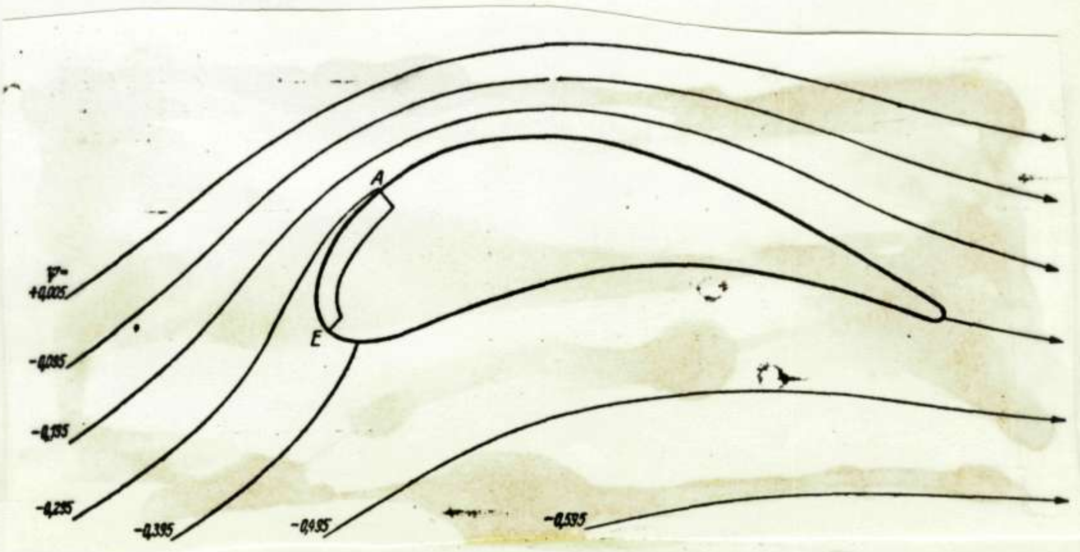

Fig. 8. Calculated flow pattern for flow around profile 7 with leading edge suction; sink distribution $q(\phi)$ = const from A to E, quantity coefficient $c_Q = -0.10$, angle of attack $\alpha = 10°$.

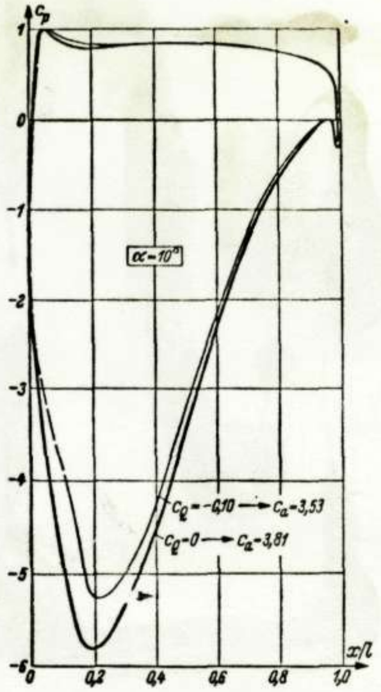

Fig. 9. Pressure distribution $c_p =$ $= (p - p_\infty)/(\frac{\rho}{2}W_\infty^2)$ at profile 7 during flow without suction and with leading edge suction in accordance with Fig. 8; $\alpha = 10°$.

peak by means of the leading edge suction with $c_Q = -0.10$. Sucked off quantities are much smaller for boundary layer suction, so that changes in potential flow due to suction should not be of any importance there.

Flow Separation

The calculated potential representation of flow separations is another interesting application of the method. Think of the dead water area filled with the liquid emitted from the profile. It is assumed to have been furnished by sources located on the contour. The source distribution is to be selected in such a way that at "dead water boundaries" close to the profile a nearly constant pressure prevails which is then to be regarded as applying to the entire dead water. By this means, the dead water pressure and the displacement effect of the dead water on the external flow of the theoretical calculation are to be made accessible.

At first, it might seem surprising that dead water flows, where friction plays a very decisive role in their formation, should be considered at all as computable in terms of potential, i.e., without friction. However, friction is taken into account to the extent of acknowledging a dead water as existing at all and also meeting a condition for the dead water boundaries that corresponds to the "reality of friction." Inside the dead water, it is of course not possible to determine the actual flow by means of our calculated potential method; it can, however, be done at the dead water boundaries and outside the dead water. The only assumption is that at the dead water boundaries and outside the dead water, the flow behaves like a potential flow with the boundary condition that from certain points on (the separation points), the pressure along as yet unknown boundary lines (the dead water boundaries) is nearly constant in the vicinity of the profile. The lines are calculated in terms of potential as boundary lines of a quantity of liquid emerging from the profile.

With such a potential flow, the "dead water" will always extend to infinity, in which case the pressure will asymptotically approach p_∞, whereas a real dead water has a finite range, and experience has shown that a reduced pressure prevails in a dead water. However, it is only necessary to correctly imitate the dead water in the vicinity of the profile by means of an outflow, since the shape of the dead water at some distance from the profile should no longer have any noticeable influence on the flow at the profile. However, by limiting oneself to the immediate vicinity of the profile, it is quite possible, as will be shown, to correctly imitate the dead water.

First, in the case of a flow separation, the angle of attack α and the points of separation -- possibly on the basis of a preceding boundary line computation -- can be regarded as given. A certain form and position of the source distribution between the points of separation will then furnish a certain "dead water region" that in general will not as yet meet the conditions of constant pressure at the dead water boundaries. The comprehensive study shows first of all that the shape of the "dead water" can be strongly influenced by the form and position of the source distribution. Finally, further experiments showed that the best way to attain nearly constant pressure at the separation lines close to the profile is by locating a constant source distribution between the two points of separation close to these points. It is still necessary though to systematically vary the total quantity of outflow (by means of the superposition factor g) and the strength of the circulation flow to be superposed (by means of the superposition factor c) until the specified condition close to the profile has been fulfilled as much as possible. Now, the superposition of the four basic flows by factors c and g, found as noted, and factors a and b, already fixed by the angle of attack α, yield the velocity and also the pressure distribution on the profile outside the dead water. A constant pressure is assumed for the dead water, i.e., the pressure determined for the separation lines is transferred to the profile.

As noted, the points of separation must be known for a computation of flow separations in terms of potential. A theoretical determination of the points of separation by means of a combination of the method under consideration and boundary line computations should be feasible. However, in order to arrive at first /63 comparisons between theory and measurements and consequently to eliminate unavoidable uncertainties in the theoretical determination of the points of separation, the points of separation in the following examples were taken from measurements (break in pressure distribution).

Figure 10 presents a comparison between theory and a measurement [12] for a flow separation on profile NACA 2412. The pressure distribution for a potential flow without separation has also been plotted in this diagram.

A further comparison with measurements was undertaken by K. Kraemer [13] on profile Gö 801. In Fig. 11 a comparison between theory and measurement with and without separation has been plotted.

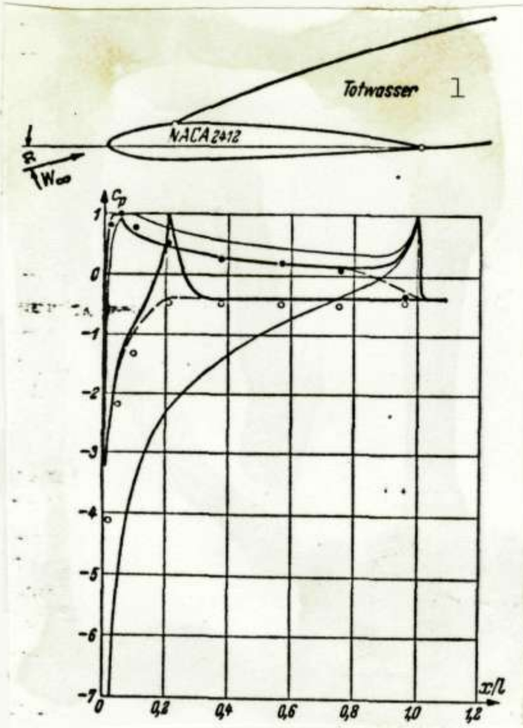

Fig. 10. Pressure distribution $c_p = (p - p_\infty)/(\frac{\rho}{2}W_\infty^2)$ on profile NACA 2412 with flow separation.
—— Theory without separation $\alpha = 16.3°$ yields $c_a = 2.09$
▬▬ Theory with separation at $x/l = 0.21$, $\alpha = 16.3°$ yields $c_a = 0.00$
--- Estimated transitions for theory with separation;
● O Measurement for rectangular wing without vertical fins with $\Lambda = 5$, $Re = 2.7 \cdot 10^6$, $\alpha_g = 17.9°$ yields in cross section: $\alpha = 16.3°$, $c_a = 0.95$.

Key: 1. Dead water

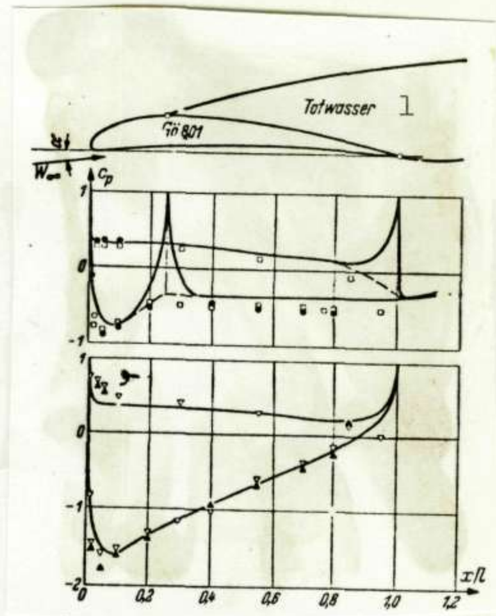

Fig. 11. Pressure distribution $c_p = (p - p_\infty)/(\frac{\rho}{2}W_\infty^2)$ on profile Gö 801 with separated and with adjacent flow. Top diagram:
—— Theory with $\alpha = 8.1°$ and separation at $x/l = 0.25$ yields $c_a = 0.63$ and $c_{wp} = 0.087$.
● □ Measurement by Kraemer, $Re = 3.2 \cdot 10^4$, $Re = 4.2 \cdot 10^4$, $\alpha = 8.1°$; $c_a = 0.61$ and $c_{w\infty} = 0.085$.
Bottom diagram:
∇ ▲ Measurements by Kraemer, $Re = 1.47 \cdot 10^5$, $Re = 4.2 \cdot 10^5$, $\alpha = 4.3°$, $c_a = 1.19$.

Key: 1. Dead water

An especially good consistency of measuring values occurs in both cases with regard to pressure distribution on the pressure side. The theoretical dead water pressure also comes quite close to the measured one. Greater deviations occur on the pressure and suction side in the vicinity of the points of separation. The points of separation are points of stagnation at constant source distribution in the potential theory. For this reason, c_p is always equal to 1. However, this is not logical from a physical standpoint and it is, therefore, better to revert to estimated curves for the theoretical dead water pressure (dotted curves in Figs. 10 and 11). In that case there remains a certain amount of uncertainty.

Lift coefficients have also been given in Figs. 10 and 11; in this respect also there is good consistency of measuring values between theory and measurement.

The theoretical lift coefficient was calculated from $c_a = 4\pi c$ (Eq. (9c)) after the superposition factor for pure circulation flow c had been found in the noted manner.

The theoretical pressure drag coefficient c_{wp} which had also /64 been given in Fig. 11 was determined by means of formula:

$$c_{wp} = c_{xp} \cos \alpha + c_{yp} \sin \alpha ,$$

in which c_{xp} or c_{yp} are the coefficients of the pressure forces in the x or y direction that were obtained by integration of the dimensionless pressure distribution plotted against y/l or x/l. Frictional resistance must be added to pressure drag ($c_{wp} = 0.087$) which, however, in the present case is of no great moment as compared to the pressure drag.

Flow Around an Airfoil with a Jet Flap

The application of the method to arbitrary jet flap flows is somewhat difficult. A flow of this type with blowing out at the rear part of the pressure side is shown in Fig. 12 and the corresponding pressure distribution in Fig. 13. However, with a given angle of attack and two stagnation points (jet width at profile),

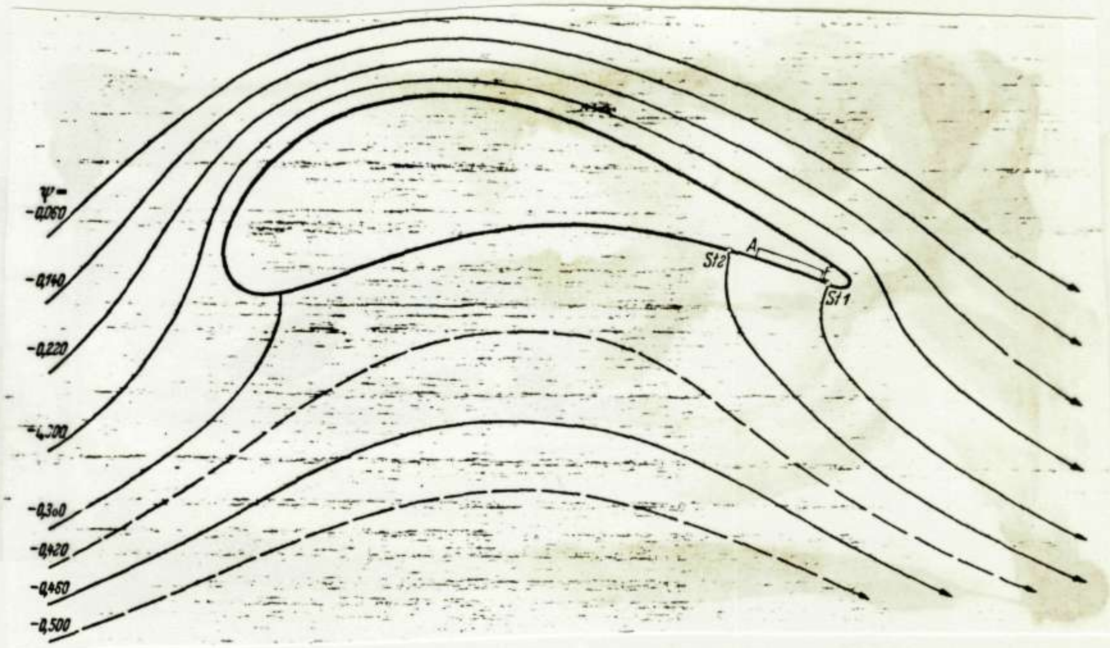

Fig. 12. Calculated flow pattern for flow around profile 7 with "jet flaps"; source distribution $q(\phi) =$ $=$ const from A to E, $\alpha = 0°$ and stagnation points St1 and St2 given; this yields: quantity coefficient of blowing $c_Q = 0.050$.

the total emitted quantity can only be changed within narrow limits by the form and position of the source distribution. It is especially difficult to readily obtain flows with large quantities of outblow at small outblow slits. Such flows certainly show great velocity jumps (vortex distributions) at the jet boundaries which at first were not incorporated in the method. It would be possible to add such vortex distributions. To be sure, where the jet boundaries would have to be applied is unknown to begin with. However, it is perhaps possible to find the way by means of iteration.

5. Summary and Outlook

A method of computation has been developed for computing plane incompressible potential flows around arbitrary thick, cambered profiles with continuous or discontinuous blowing or suction. It works with source and vortex distributions on the contour of the profile and in the interior of the profile. An

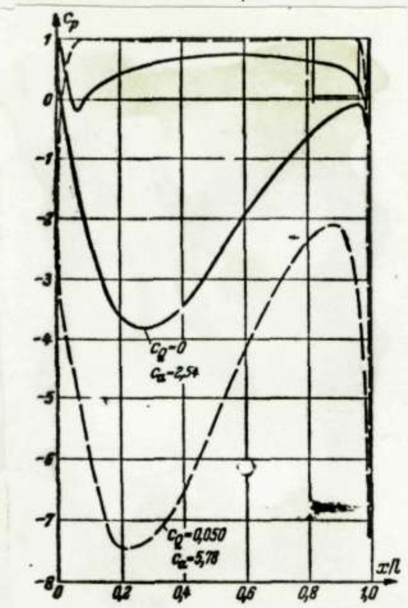

Fig. 13. Pressure distribution $c_p = (p - p_\infty)/(\frac{\rho}{2}W_\infty^2)$ on profile 7 with $\alpha = 10°$. —— Without jet flap; --- With "jet flap" in accordance with Fig. 12.

integral equation for the vortex distribution on the contour of the profile is arrived at, the solution of which is reduced to a linear set of equations. Finally, the method yields the velocity and pressure distribution on the contour of the profile and the flow-stream function for plotting of the flow pattern.

The method is well suited for use in digital electronic computers and was programmed for the IBM 650. A series of example computations was carried out. About 1 hour of computing time is required for the velocity and pressure distribution of a flow, about 1.5 hours for the flow pattern.

The practicability of the method was established for the circular cylinder by comparing the velocity distribution with the exact solution, and on some thick, cambered profiles by comparison of the theoretical pressure distribution with measurements.

The following perspectives present themselves for a practical application of the method. A change in the potential flow by means of suction is readily obtained. A representation of flow separations is possible but requires a trial-and-error method in order to meet boundary conditions at the boundaries of the /65 "dead water zone." An application of the method for flows around profiles with jet flap will generally not be possible unless the jet border is also equipped with a vortex distribution and possibly also with a sink distribution.

REFERENCES

1. F. Ehlers, "On the Change in Lift and Pressure Distribution on Wings with Boundary Layer Bleed by Means of a Sink Effect," AVA Report 45 W 15 (1945).

2. C.B. Smith, J. Aero. Sci. 16, 581 (1949).

3. W.T. Lord, "The Incompressible Potential Flow Past Two-Dimensional Airfoils with Arbitrary Surface," Suction ARC Current Paper 56 (1950).

4. J.M. Davidson, J. Roy. Aero. Soc. 60, 45 (1956).

5. W. Jacobs, Z. Flugwiss. 5, 253 (1957).

6. G. Jungclaus, Z. Flugwiss. 5, 172 (1957).

7. R. Eppler, J. Rat. Mech. Anal. 3, 591 (1954).

8. L. Prandtl, Tragflügeltheorie [Theory of Airfoils], Vol. I, Nachr. d. K. Gesellsch. d. Wissensch., Göttingen, Math.-Phys. Klass, 1918, p. 451.

9. W. Prager, Phys. Z. 29, 865 (1928).

10. E. Martensen, "Calculation of Pressure Distribution on Thick Grid Profiles by Means of Fredholm's Integral Equations of the Second Degree," Mitt. MPI Ström. Forsch. u. Aerodyn. Vers. Anstalt. (23), 1 (1959).

11. E. Martensen and K. v.Sengbusch, Arch. Rat. Mech. Anal. 5, 46 (1960).

12. F.W. Riegels, Aerodynamische Profile [Aerodynamic Profiles], Munich 1958.

13. K. Kraemer, "Investigation of an Airfoil in the Wind Tunnel with Sub- and Supercritical Reynolds Numbers," AVA Report 58-01 (1958).